Available online at www.sciencedirect.com
ScienceDirect
Trans. Nonferrous Met. Soc. China 21(2011) 477−481
Transactions of Nonferrous Metals Society of China
www.tnmsc.cn

Microstructure and mechanical properties of Mg-Li alloy after TIG welding

LIU Xu-he[1], GU Shi-hai[1], WU Rui-zhi[1], LENG Xue-song[2], YAN Jiu-chun[2], ZHANG Mi-lin[1]

1. Key Laboratory of Superlight Materials and Surface Technology of Ministry of Education, Harbin Engineering University, Harbin 150001, China;
2. State Key Laboratory of Advanced Welding Production Technology, Harbin Institute of Technology, Harbin 150001, China

Received 6 April 2010; accepted 29 September 2010

Abstract: Tungsten inert gas weld was carried out on super-light magnesium-lithium alloy plates with a thickness of 2 mm, using argon gas as a protecting atmosphere. The microstructure and mechanical properties of the welded joints were investigated. The results indicate that the microstructure in the fusion zone is fine, and the microstructure in the heat-affected zone is coarser than the parent metal. The tensile strength of the welded joint is about 84% that of the parent metal. The fracture occurs in a mixed type of toughness and brittleness in the heat-affected zone. During the welding process, aluminum and cerium are enriched at grain boundaries in the fusion zone.

Key words: Mg-Li alloy; TIG welding; microstructure; mechanical properties; segregation

1 Introduction

Magnesium alloys have low density, high-specific strength, excellent dimensional stability and good energy absorption. These alloys are also recyclable, making them a kind of green metallic structural material for the 21st century[1−2]. Mg-Li alloys with a density smaller than normal magnesium alloys have attracted much attention among researchers for their potentially broad applications in aerospace, transportation, electronic and military industries[3]. Consequently, researchers have done a lot of work on the welding of magnesium alloy[4−6], as joints are important for advanced materials with wide applications.

Because Mg alloys have a low melting point, high thermal conductivity, electrical conductivity and thermal expansion coefficient, they are chemically active and readily oxidized[7−8]. ASAHING[6] pointed out that due to the deformation during welding process, the solidification cracks of TIG welded magnesium alloy were restrained[9−10]. CAO et al[11] found that many difficulties, such as coarse grains, oxidation, volatilization and thermal cracking, occur during welding because magnesium alloys have a low melting point and large thermal conductivity, electrical conductivity and thermal expansion coefficient. Mg-Li alloys have similar problems, and as their applications increase, the welding of these materials causes great concerns.

In this work, a superlight magnesium-lithium alloy is welded by tungsten inert gas (TIG) welding using a homogeneous wire. The microstructure is analyzed and the mechanical properties of the welded joint are discussed. The results provide an effective theoretical and experimental basis for expanding the application of magnesium-lithium alloy.

2 Experimental

The alloy used in this experiment was melted in a vacuum intermediate induction furnace under the protection of argon atmosphere. The ingot was then extruded with an extrusion ratio of 16 at 653 K and rolled at 473 K. The chemical composition of the

Foundation item: Project (51001034) supported by the National Natural Science Foundation of China; Project (208181) supported by the Key Project of Chinese Ministry of Education; Projects (2008AA4CH044, 2009AA1AG065, 2010AA4BE031) supported by the Key Project of Science and Technology of Harbin City, China; Project (HEUCF101001) supported by the Fundamental Research Funds for the Central Universities, China

Corresponding author: WU Rui-zhi; E-mail: Ruizhiwu2006@yahoo.com

DOI: 10.1016/S1003-6326(11)60739-5

magnesium-lithium alloy plates used in this experiment is shown in Table 1. The density of the alloy was tested by Archimedes' method and found to be 1.45 g/cm^3. The tensile strength of the base metal before welding was 160.8 MPa and the elongation was 34.7%. The thickness of the base metal was 2 mm before welding bevels was processed as shown in Fig.1 on the plates.

Table 1 Chemical composition of Mg-Li alloy (mass fraction, %)

Li	Al	Zn	Ce	Mg
10.36	2.69	0.91	0.81	85.23

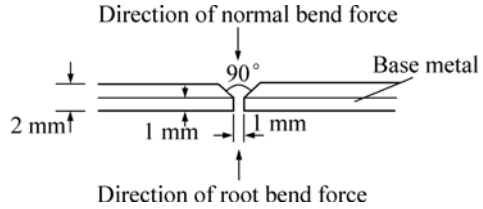

Fig.1 Schematic diagram of bevel

Before welding, the surfaces of the specimens and wires were cleaned. The specific process involved sanding, washing with acetone, washing with water, washing with alkali, washing with water, washing with acid, washing with water and drying, consequently.

In order to prevent dislocations during the welding process, the two pieces were fixed. There were indentations in the back of the sizing block, which were used to control the penetration and shape.

The parameters of the welding procedure are shown in Table 2. In order to reduce overheating and prevent burn-through, a high welding speed was used in the process.

Table 2 Parameters of welding procedure

Welding current/A	Welding speed/ (cm·min^{-1})	Gas flow/ (L·min^{-1})	Welding arc voltage/V
80	30	13	18

After welding, the sample was cut perpendicularly to the welding seam. These specimens were then prepared using standard metallographic procedures. The specimens were etched by a 2% nital for 10−30 s until the microstructure was revealed. The microstructure was subjected to optical and scanning electron microcopy and the distribution of the alloying elements was measured using energy dispersive X-ray spectroscopy.

After removing the residual part of the coronal zone, the plates were machined into tensile specimens according to the ASTM E8M-04 standard procedure. The schematic diagram of tensile specimens is shown in Fig.2, and the tensile test was brought out at a speed of 5 mm/min on five specimens. Bending properties were also tested.

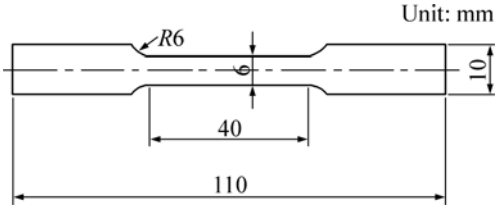

Fig.2 Dimensions of tensile specimen

3 Results and discussion

3.1 Macro-morphology of welding seam

The macro-morphology of the welding seam is shown in Fig.3. There are no macroscopic irregularities, such as weld beadings or crater cracks.

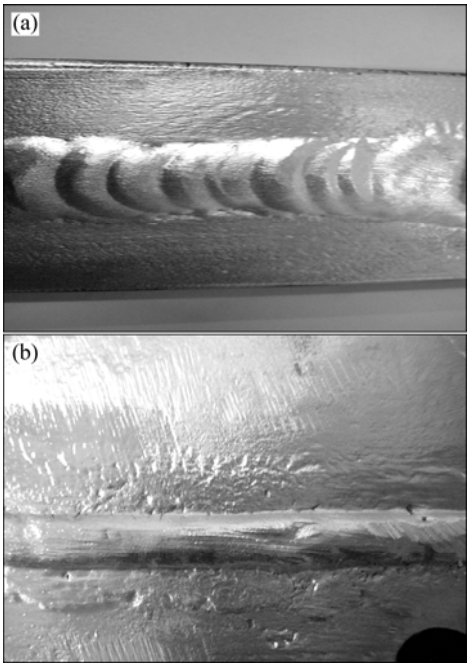

Fig.3 Macro-morphology of welded seam: (a) Front face; (b) Back face

3.2 Microstructure of welded joint

The TIG-welded joint included a fusion zone, a heat-affected zone (HAZ) and a base metal zone. The microstructure of the welded joint is shown in Fig.4. The base metal is composed of single phase (β phase) with equiaxed grains which are not uniform. The microstructure in heat-affected zone is coarser than that in the parent metal. In Fig.4(c), the microstructure of the fusion zone exhibits refined grains. As shown in Fig.4(d), the base metal and welding seam are fused well and the structure is tight.

The microstructures in different areas are not uniform, which are mainly related to the TIG welding

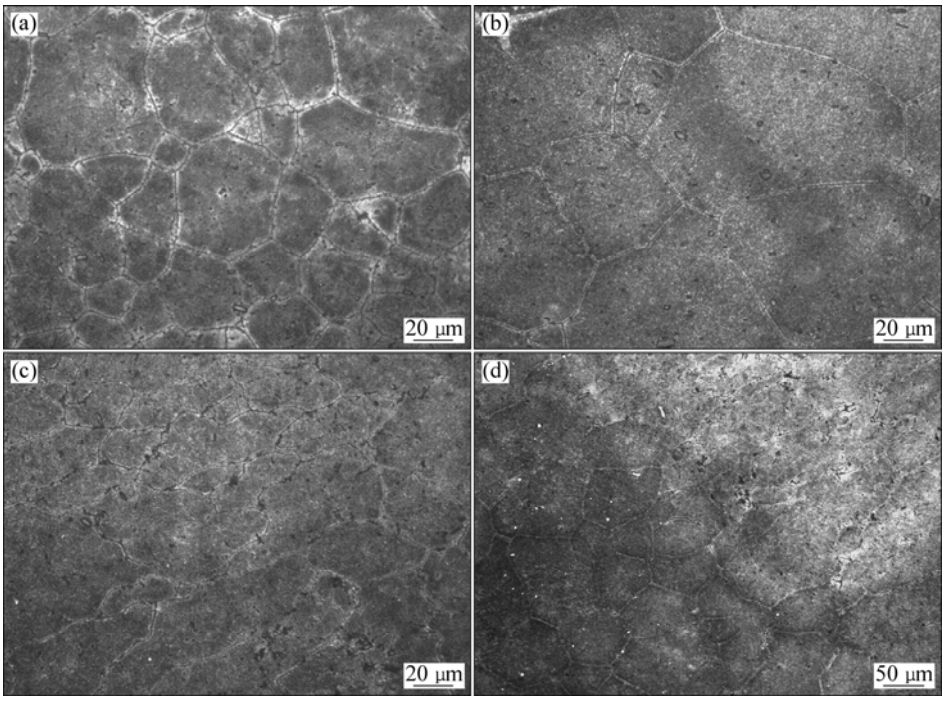

Fig.4 Microstructures of welded joint: (a) Base metal; (b) HAZ; (c) Fusion zone; (d) Junction of base metal and heat-affected zone

thermal cycle process and the physical properties of magnesium alloys. During the welding process, the metal in the fusion zone absorbs a large amount of heat and melts, and then quickly solidifies because the thermal conductivity coefficient of magnesium alloy is high (154 W/(m·K))[12−13]. On the other hand, the pulses in the welding process contribute to the rapid solidification of the metal. Therefore, the microstructure of the fusion zone is refined. During the welding process, because the melting point of magnesium alloys is low (usually 500−600 °C)[14−15], the heat-affected zone is wide and easily overheated, so the absorbed heat promotes grain growth, resulting in coarser grains in the heat-affected zone. After rolling deformation, the stored energy is relatively high and the grains are extremely unstable. Therefore, the grains grow rapidly when they are heated.

3.3 Mechanical properties of TIG welded plate

The mechanical properties of the TIG welded specimens and the base metal are given in Table 3. The tensile strength of the TIG welded plate is 84% that of the parent metal.

Table 3 Tensile properties of Mg-Li alloys

Sample	Tensile strength/MPa	Fault location
Base metal	170.75	Middle of sample
Welded plate	143.76	Welding zone

According to Fig.4, the grains in the heat-affected zone are clearly coarser than those in the fusion zone and the base metal. These coarse grains result in a decrease of mechanical properties. As proved by the tensile test, fractures occurred in the heat-affected zone, which indicates that coarse grains are the main reason for the decrease in the mechanical properties of the weld plate.

Table 4 shows the results of the bend test. The angle of the normal bend test and the root bend test approach show similar ductility in the front and back. Therefore, it is confirmed that there is no front/back difference in properties in this welding procedure.

Table 4 Result of bend test

Bending mode	Angle/(°)
Front bend	30.3
Back bend	30.1

3.4 Fracture analysis

According to the macro-fracture morphology, the base metal fractures in the middle of the specimen, the angle between the fracture plant and the tensile direction is 45°. The fracture of the TIG welded sample occurs in the heat-affected zone, and the facture face is rough and dark. There is no obvious necking before failure.

Figure 5 shows the fractographs of the base metal and the TIG welded specimen. The fracture microstructure of the base metal consists of dimples, which is a typical micro-void coalescence fracture. The fracture microstructure of TIG welded sample is composed of dimples and cleavage planes, which is characteristic of a mixed-type fracture. This is

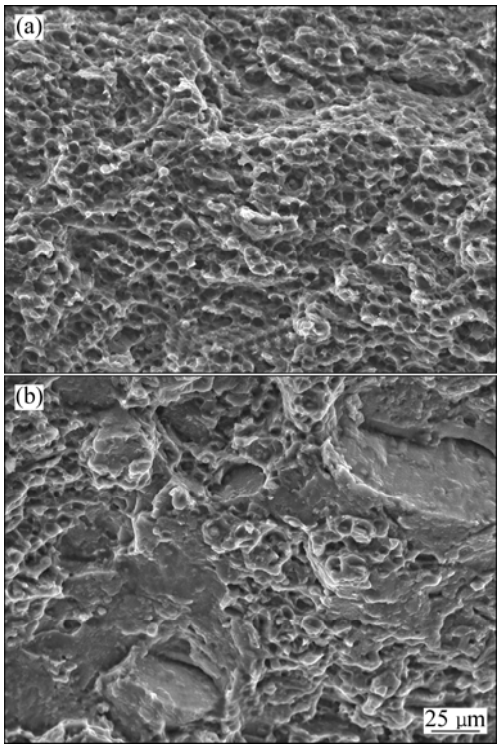

Fig.5 Fractographs of base metal (a) and TIG welded sample (b)

caused by the change of the microstructure.

3.5 Composition analysis

The microstructure of the compouds is shown in Fig.6. The compositions in the fusion zone were analyzed by EDS, and the results are shown in Table 5. The compound mainly consists of magnesium, aluminum and cerium, and the content of zinc is zero. The solid solubility of cerium in magnesium is 0.5%. During solidification, most of the cerium reacts with other elements to form compounds[16]. The electronegative difference between the magnesium and cerium is 0.1, while that between aluminum and cerium, zinc and cerium is about 0.4. Cerium should first react with aluminum. The solid solubility of zinc in magnesium is large. The content of zinc in this work is lower than 1%, and it can be assumed that all the zinc is soluted in magnesium. Considering that magnesium is the matrix, the molar ratio of aluminum to cerium is about 2:1, so it can be predicted that the compound is Al_2Ce.

During the welding process, the alloy in the welding zone undergoes re-solidification. Therefore, segregation may occur.

As shown in Table 5, the contents of magnesium and zinc at the intracrystalline phases (Point *A*) are higher than those at grain boundaries (Point *B*), and the contents of aluminum and cerium at the intracrystalline phase are lower than those at grain boundaries. This illustrates that during re-solidification, aluminum and cerium enrich at the front of the solid-liquid interface after reacting, so that the contents of aluminum and cerium in the matrix decrease, leading to under cooling and refinement of grains in the weld zone.

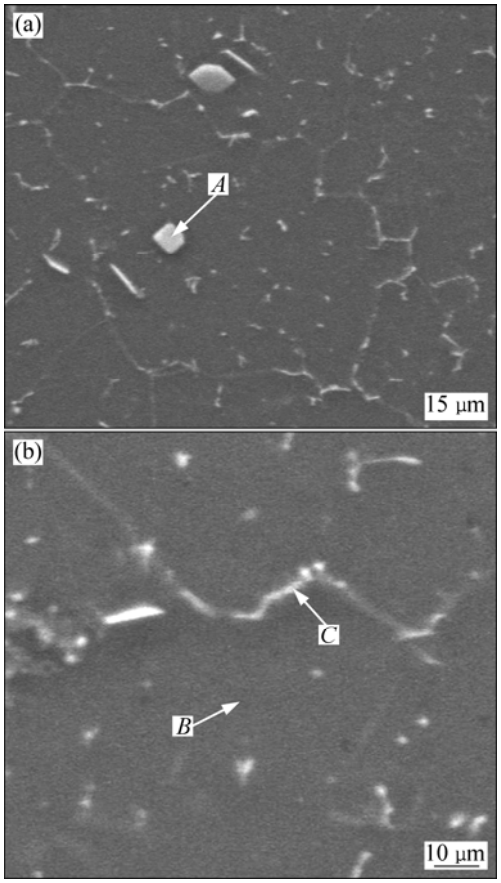

Fig.6 SEM images of compound in fusion zone (a) and grain boundary and intracrystalline phase (b)

Table 5 Microanalysis of positions in Fig.6 (molar fraction, %)

Element	Point *A*	Point *B*	Point *C*
Mg	46.11	88.76	83.40
Al	34.97	0.21	1.65
Zn	0	0.79	0.41
Ce	18.62	0.20	2.40

4 Conclusions

1) Using the same material as wire, a TIG weld was implemented on the Mg-10.36Li-2.7Al-0.91Zn-0.81Ce alloy. There are no obvious weld defects.

2) The microstructure in the fusion zone is fine, while that in the heat-affected zone is coarse. The heat-affected zone is the weaker part of the weld plate.

3) The tensile strength of the TIG welded plate is 143.73 MPa, which is 84% that of the parent metal. Fractures occurred in the heat-affected zone, which exhibits a mixed-mode fracture of ductile-brittle.

4) The segregation and enrichment of Al and Ce are

found at the grain boundaries.

References

[1] SANSCHAGRIN A, TREMBLAY R, ANGERS R, DUBE D. Mechanical properties and microstructure of new magnesium-lithium base alloys [J]. Materials Science and Engineering A, 1996, 220(1−2): 69−77

[2] ZHANG Mi-lin, WU Rui-zhi, WANG Tao, LIU Bin, NIU Zhong-yi. Microstructure and mechanical properties of Mg-*x*Li-3Al-1Ce alloys [J]. Transactions of Nonferrous Metal Society of China, 2007, 17(s1): s381−s384.

[3] WU Rui-zhi, DENG Yong-shu, ZHANG Mi-lin. Microstructure and mechanical properties of Mg-5Li-3Al-2Zn-*x*RE alloys [J]. Journal of Materials Science, 2009, 44(15): 4132−4139.

[4] SU S, HUANG J, LIN H, HO N. Electron-beam welding behavior in Mg-Al based alloys [J]. Metallurgical and Materials Transactions, 2002, 33(5):1641−1673.

[5] MARYA M, EDWARDS G LIN S. An investigation on the effects of gasses in GTA welding of a wrought AZ80 magnesium alloy [J].Welding Journal, 2004(7): 203−212.

[6] ASAHING T, TOKISUJE H, KATOH K. Solidification crack sensitivity of TIG welded AZ31 magnesium alloy [J]. Journal of Japan Institute of Light Metals, 1999, 49(12): 595−599.

[7] ZHU Tian-ping, CHEN Zhan W, GAO Wei. Incipient melting in partially melted zone during arc welding of AZ91D magnesium alloy [J]. Materials Science and Engineering A, 2006, 416(1−2): 246−252.

[8] MUNITZ A, COTLER C, STERN A, KOHN G. Mechanical properties and microstructure of gas tungsten arc welded magnesium AZ91D plates [J]. Materials Science and Engineering A, 2001, 302: 68−73.

[9] LIU Sheng-xin, CHEN Yong, WANG Xi-he, LIU Xiao-fang, LI Qing-kui, GUAN Shao-kang. Study on microstructure and mechanical properties of He-Ar mixed gas TIG welded joint for AZ31 magnesium alloy plates. [J] Metal Hotworking Technology, 2007, 6(7): 12−14.

[10] ZHENG Rong, LIN Ran. TIG welding of thin plate in AZ31B Mg alloy [J]. Welding and Joining, 2003, 4: 43−44.

[11] CAO X, JAHAZI M, IMMARIGEON J, WALLACE W. A review of laser welding techniques for magnesium alloys [J]. Journal of Materials Processing Technology, 2006, 58(8): 188−204.

[12] WANG Xi-he, LIU Sheng-xin, CHEN Yong, KUANG Ying-huan, GUAN Shao-kang, NIU Ji-tai. Effect of He-to-Ar ratio on weld ability of TIG of AZ31 magnesium alloy [J]. Light Alloy Fabrication Technology, 2006, 34(12): 43−45. (in Chinese)

[13] SUN Si-quan, WANG Li-jun. Mechanical properties of magnesium alloys welded joints [J]. Welding Technology, 2004 33(5): 110−115.

[14] DING Wrn-bin, JIANG Hai-yan, ZENG Xiao-qin, YAO Shou-shan. Progress in welding technology of magnesium alloy [J]. Light Alloy Fabrication Technology, 2005, 32(3):123−126. (in Chinese)

[15] WANG Zhe, LI Dao-gang, WANG Guo-ping. Analysis of structure and property of cast Mg alloy AZ91 weld joints [J]. Modern Welding, 2008, 6: 26−28.

[16] WANG Tao, ZHANG Mi-lin, WU Rui-zhi. Microstructure and properties of Mg-8Li-1Al-1Ce alloy [J]. Materials Letters, 2008, 62: 1846−1848.

一种镁锂合金的 TIG 焊接组织与力学性能

刘旭贺[1]，顾世海[1]，巫瑞智[1]，冷雪松[2]，闫久春[2]，张密林[1]

1. 哈尔滨工程大学 超轻材料与表面技术教育部重点实验室，哈尔滨 150001
2. 哈尔滨工业大学 现代焊接生产技术国家重点实验室，哈尔滨 150001

摘　要：以氩气为保护气体，用同种合金的焊丝对一种 2 mm 厚的超轻镁锂合金板进行 TIG 焊接，研究焊接接头的显微组织和力学性能。结果表明，与母材相比，焊缝区晶粒细小，热影响区晶粒粗大。焊件的抗拉强度为母材的 84%，断裂发生在热影响区，属于韧-脆混合性断裂。焊接后，焊缝区的 Al 和 Ce 在晶界处富集。

关键词：镁锂合金；TIG 焊接；显微组织；力学性能；偏析

(Edited by FANG Jing-hua)